Available online at www.sciencedirect.com
SCIENCE @ DIRECT®

Journal of the European Ceramic Society 24 (2004) 2649–2656
www.elsevier.com/locate/jeurceramsoc

Thermodynamic vaporization studies of the manganese oxide–yttria stabilized zirconia (YSZ) solid solution

Aleksandra Matraszek[a], Miroslaw Miller[b], Lorenz Singheiser[a], Klaus Hilpert[a,*]

[a]Research Center Jülich, Institute for Materials and Processes in Energy Systems, 52425 Jülich, Germany
[b]Wroclaw University of Technology, 50 370 Wroclaw, Poland

Received 28 May 2003; accepted 20 September 2003

Abstract

Samples of the compositions $(Zr_{0.85}Y_{0.15})_{1-x}Mn_xO_{1.93-\delta}$, $0.02 \leqslant x \leqslant 0.25$, were prepared and characterized by means of XRD and SEM/EDX analysis. The vaporization of manganese oxide from the samples with $x \leqslant 0.18$ was studied by Knudsen effusion mass spectrometry in the temperature range of 1539–1858 K. Partial pressures of gaseous Mn, MnO, and O_2 were determined over the samples investigated and thermodynamic activities of MnO in the samples evaluated at 1700 K. Chemical and phase compositions of the samples were determined after the vaporization measurements and the results obtained were correlated with the obtained values of the thermodynamic activity of MnO. The thermodynamic activities determined belong to the solubility range of manganese oxide in yttria stabilized zirconia. Moreover, thermodynamic data on the vaporisation of pure MnO(s) resulted.
© 2003 Elsevier Ltd. All rights reserved.

Keywords: Chemical properties; Fuel cells; Vaporization; ZrO_2

1. Introduction

ZrO_2 base ceramics are of great importance in many applications such as high temperature electrolytes in fuel cells, oxygen gas sensors, heat-resistant linings of high temperature furnaces, biomaterials, and others.[1–3] Zirconia stabilized with 8 mol% of yttria (8YSZ) is a well known established solid electrolyte used in electrochemical devices.[3,4] The chemical composition of 8YSZ was proposed by different groups in order to get high oxygen ion conductivity[4] and due to the stabilization of the cubic crystal structure in a large temperature range. The latter is important for the production process of the electrolyte which is typically performed at 1700 K and for the operating temperature of electrochemical devices, which amounts to about 1100–1200 K in case of solid oxide fuel cells (SOFC). In spite of this, contradictory data are available on the phase diagram of the Y_2O_3–ZrO_2 system.[5] Some authors (e.g. Ref. [4]) explain the reduction of the ion conductivity of 8YSZ at high temperature by the change of the phase composition of the material. According to this explanation, the cubic phase is a metastable one and can at least partially be transformed into the tetragonal phase under thermodynamic equilibrium.

Perovskites on the basis of $LaMnO_3$ are widely used as cathode material in SOFCs [3,6] which is in direct contact with the electrolyte material. Diffusion of Mn cations from the cathode into electrolyte was observed by different authors.[7,8] Yokokawa et al.[9] considered the thermodynamic aspects of the $LaMnO_3$ reactivity with 8YSZ under SOFC operating conditions. The same authors explain the fast diffusion of the Mn ions into 8YSZ by the partial reduction of the Mn valency from +3 in the perovskite phase down to +2 in the 8YSZ/MnO solid solution,[10] the latter being thermodynamically more favorable. The $La_2Zr_2O_7$ phase can be an additional product of the diffusion processes at the $LaMnO_3$/8YSZ interface.[11]

According to different studies, the maximum solubility of Mn in 8YSZ amounts to 15 mol% at 1773 K .[12–15] Substitution of Mn ions for Y/Zr in the 8YSZ phase stabilizes the cubic structure.[14] Mixed +3/+2 valency of Mn in the solid solution YSZ/MnO results by different investigations.[9,15,16]

Vaporization of the solid solution Y_2O_3–ZrO_2 was studied by Knudsen effusion mass spectrometry at temperatures of 2550–2900 K.[17] In contrast to this, the

---

* Corresponding author. Tel.: +49-2461-613700; fax: +49-2461-613299.

E-mail address: k.hilpert@fz-juelich.de (K. Hilpert).

0955-2219/$ - see front matter © 2003 Elsevier Ltd. All rights reserved.
doi:10.1016/j.jeurceramsoc.2003.09.015

vaporization of pure MnO(s) was investigated at temperatures of 1618–1815 K using the same method.[18,19] It is interesting to note that the Mn_3O_4(s) phase, stable in air, decomposes into MnO(s) and O_2(g) on heating under low oxygen partial pressure as it is present in a Knudsen cell in the course of vaporization studies using Knudsen effusion mass spectrometry. MnO(s) vaporizes forming the gaseous species Mn, MnO, and O_2.

The vaporization of MnO from the solid solution 8YSZ/MnO is studied by Knudsen effusion mass spectrometry in this work for the first time. The determination of the thermodynamic activity of MnO in this solution for different Mn concentrations is the aim of this study. The thermodynamic activities are also of interest in order to understand the chemical interactions at the interface [(Mn containing cathode)/8YSZ] of a SOFC.

2. Experimental

2.1. Sample preparation

Nine $(Zr_{0.85}Y_{0.15})_{1-x}Mn_xO_{1.93-\delta}$ samples (denoted as 8YSZ 100*x*Mn) of different chemical composition listed in Table 1 were prepared by solid state chemical reaction from 8YSZ powder (purity 99%) supplied by Tosoh, Japan, and from MnO (purity 99%) supplied by Heraeus, Germany. Stoichiometric amounts of components were mixed in acetone, pressed into pellets, and annealed in air at 1673 K for 16 h. The calcined pellets were ground again in an agate mortar, pressed into pellets, and annealed at 1673 K for 32 h.

2.2. Mass spectrometric measurements

The vaporization studies of the samples were carried out by Knudsen effusion mass spectrometry at Research Center Jülich (see e.g. Refs [20,21]). The instrument of the MAT 271 type was supplied by Finnigan MAT, Bremen, Germany, and is completely computer-controlled. The vapor species were ionized with an emission current of 1 mA and an electron energy of 70 eV. Knudsen cells made of tungsten and lined completely with iridium were employed in the measurements. Temperatures were measured by an automatic pyrometer of the ETSO-U type supplied by Dr. Georg Maurer GmbH, Kohlberg, Germany, and calibrated using the melting points of nickel, silver, gold, and platinum.

Twenty-three runs were performed in order to elucidate the vaporization of the 8YSZ 100*x*Mn samples. The initial temperature of the vaporization measurements was typically the highest temperature of a run. Decreasing measurement temperatures were then adjusted. Finally, 3–5 increasing temperatures were adjusted after reaching the lowest measurement temperature in order to show the reproducibility of the vapor pressure measurements. The same material was generally vaporized within the vaporization measurements for a sample composition. The exception was a sample of a composition 8YSZ10Mn. No MnO^+ signal could be recorded in runs 11–13 for this sample due to interfering background ion intensities. The vaporization study of this sample was, therefore, repeated in runs 14 and 15 by the use of new material. Between the runs, the samples were taken out of the Knudsen cell, ground in an agate mortar to recondition the vaporization surface, and then studied again. Details of the runs are given in Table 2.

Vaporization of pure MnO(s) was carried out within three runs in order to compare its equilibrium vapor composition with that over the 8YSZ/MnO solid solutions.

The calibration of the Knudsen cell–mass spectrometer system was performed by the vaporization of pure metals as described in Section 3.

3. Results

3.1. Chemical and phase compositions of the samples

The phase composition of the samples after the preparation was determined by XRD analysis (see Table 1).

Table 1
Chemical and phase composition of the $(Zr_{0.85}Y_{0.15})_{1-x}Mn_xO_{1.93-\delta}$ samples as prepared as well as of their residues after the vaporisation study

Sample	Nominal chemical composition, *x*	Samples as prepared		Residue of samples after the vaporisation	
		Chemical composition, *x*[a]	Phase composition	Chemical composition, *x*[a]	Phase composition
8YSZ02Mn	0.02	0.0209	8YSZ	0.0198	8YSZ
8YSZ04Mn	0.04	0.0392	8YSZ	0.0364	8YSZ
8YSZ06Mn	0.06	0.0575	8YSZ	–	8YSZ
8YSZ08Mn	0.08	0.0745	8YSZ	–	8YSZ
8YSZ10Mn	0.10	0.0854	8YSZ	0.0861	8YSZ
8YSZ12Mn	0.12	0.111	$8YSZ+Mn_3O_4$	0.109	8YSZ
8YSZ15Mn	0.15	0.139	$8YSZ+Mn_3O_4$	0.135	8YSZ + MnO
8YSZ18Mn	0.18		$8YSZ+Mn_3O_4$	0.161	8YSZ + MnO
8YSZ25Mn	0.25		$8YSZ+Mn_3O_4$		8YSZ + MnO

[a] Determined by ICP–OES, relative uncertainty ±3%

Table 2
Details of the vaporization study of the $(Zr_{0.85}Y_{0.15})_{1-x}Mn_xO_{1\cdot 93-\delta}$ samples by Knudsen effusion mass spectrometry[a]

Sample	x (nominal)	No. of run	ΔT/K	n
8YSZ02Mn	0.02	1	1670–1833	13
		2	1694–1858	13
8YSZ04Mn	0.04	3	1679–1838	16
		4	1668–1834	13
8YSZ06Mn	0.06	5	1709–1851	11
		6	1694–1824	15
		7	1683–1822	15
8YSZ08Mn	0.08	8	1661–1806	12
		9	1674–1810	15
		10	1670–1789	10
8YSZ10Mn	0.10	11	1669–1790	10
		12	1666–1797	14
		13	1649–1765	14
8YSZ10Mn	0.10	14	1539–1716	18
		15	1614–1733	13
8YSZ12Mn	0.12	16	1652–1770	13
		17	1546–1730	18
		18	1562–1743	17
8YSZ15Mn	0.15	19	1545–1726	18
		20	1545–1716	16
		21	1548–1728	18
8YSZ18Mn	0.18	22	1641–1759	13
		23	1619–1736	13
MnO(s)	-	24	1556–1687	18
		25	1599–1749	11
		26	1535–1782	17

[a] ΔT, temperature range of the different runs; n, number of measurements at the different temperatures of a run.

Fig. 1 a,b show, as an example, the XRD pattern of the samples 8YSZ04Mn and 8YSZ25Mn. Two samples, 8YSZ18Mn and 8YSZ25Mn, composed of the Mn_3O_4(s) phase in addition to the 8YSZ/MnO solid solution, were studied by SEM/EDX in order to determine the maximum solubility of MnO in the 8YSZ phase. Fig. 2 a,b show the microstructure of these samples.

MnO is depleted in the samples in the course of the vaporization measurements. The residues obtained after the last vaporization run were, therefore, characterized using XRD and chemical analysis by ICP/OES. Fig. 3 shows as an example the XRD pattern obtained before and after the vaporization study of the sample 8YSZ18Mn. The results of the chemical analysis are summarized in Table 1. No chemical analysis was carried out for the samples 8YSZ06Mn and 8YSZ08Mn after the vaporization studies due the small amount of the residues.

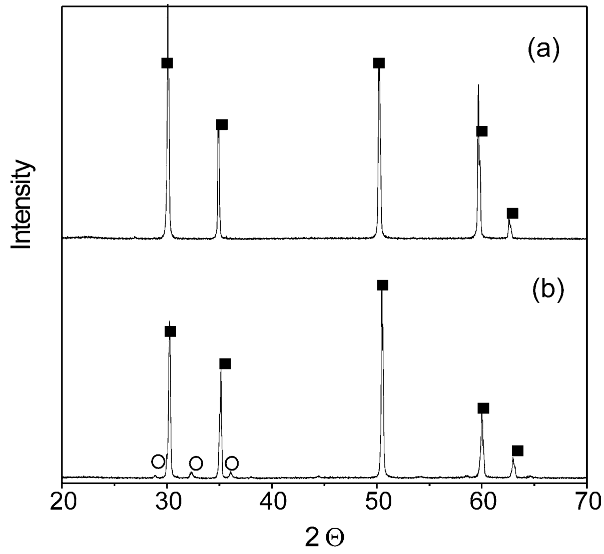

Fig. 1. XRD patterns of the samples 8YSZ04Mn (a) and 8YSZ25Mn (b) after preparation. ●, YSZ; ○, Mn_3O_4.

3.2. Ionic species and their assignment to neutral precursors

The ion species Mn^+, MnO^+, and O_2^+ were detected in the mass spectrum of the vapor over all samples listed in Table 1 as well as over MnO(s). The O^+ ion signal originating from the samples was not recorded because of interfering background ion intensities at $m/e = 16$ amu. The ions detected were assumed to originate from the respective neutrals of the same composition as reported in Refs.[18,22] Table 3 exemplifies the ion intensities corrected for isotopic distribution as measured in run 7 on vaporizing the sample 8YSZ06Mn.

3.3. Partial pressures

Partial pressures $p(i)$ of species i at the temperature T over the samples were obtained from the equation

$$p(i) = \{kT\Sigma I(i)\}/\sigma(i) \qquad (1)$$

where k and $\Sigma I(i)$ are, respectively, the pressure calibration factor and the sum of the intensities of the ions originating from the same neutral precursor i. $\sigma(i)$ is the relative ionization cross section of the species i. The values of the ionization cross sections $\sigma(i)$ given in parentheses were used for the following gaseous species i: Ag (5.35),[23] Au (6.82),[24] Ni (5.08),[25] O_2 (1.25),[26] and Mn (4.79).[27] The ionization cross section of MnO(g) was estimated as 3.40 on the basis of the experimental cross-section ration $\sigma(MO)/\sigma(M) = 0.71$ selected from the data reported by Drowart [28] for transition metals M.

The pressure calibration procedure was carried out by vaporizing pure Ag, Au, and Ni at their melting temperatures. The same cover of the Knudsen cell was used in the vaporization studies of samples and calibration substances to secure identical dimensions and geometry of the effusion orifice. In order to avoid vapor condensation inside the Knudsen cell cover its temperature was kept somewhat higher in comparison to the sample surface (about 20 K at 1700 K). The mean value of

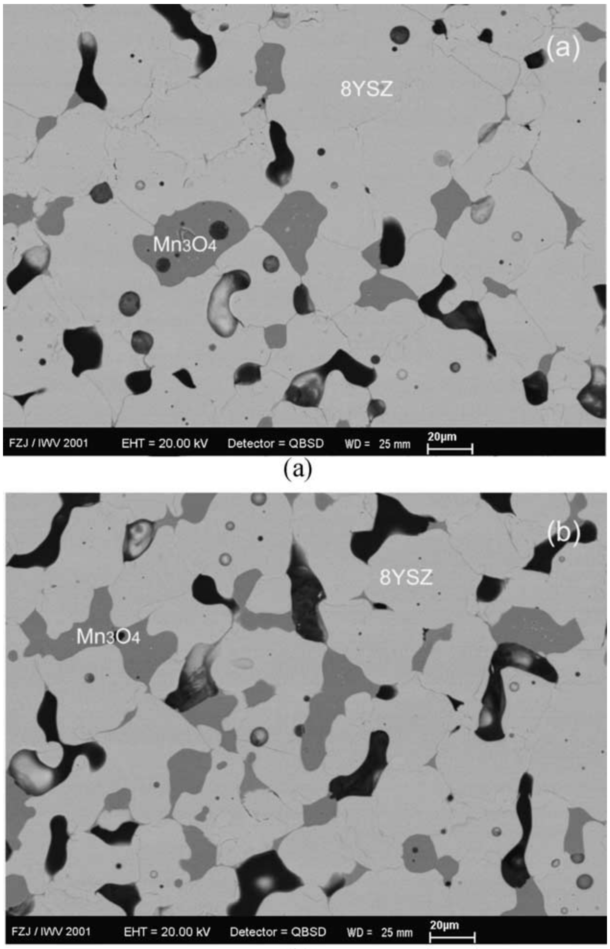

(a)

(b)

Fig. 2. SEM micrograph of the samples 8YSZ18Mn (a) and 8YSZ25Mn (b).

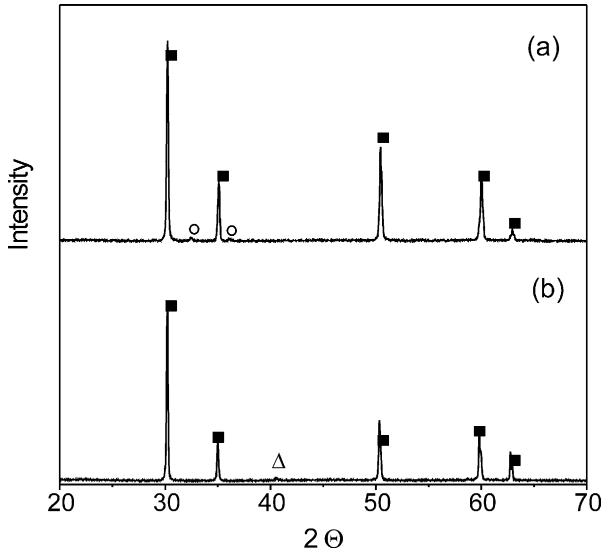

Fig. 3. XRD patterns of the sample 8YSZ18Mn before (a) and after the vaporization study (b). ●, YSZ; ○, Mn_3O_4; Δ, MnO.

Table 3

Intensities of different ions in s^{-1} determined at the different measurement temperatures upon vaporizing the sample 8YSZO6Mn in the course of run 7

T/K	$O_2(g)/O_2^+$	$Mn(g)/Mn^+$	$MnO(g)/MnO^+$
1822	1.85×10^3	1.80×10^4	1.41×10^2
1811	1.39×10^3	1.51×10^4	90.5
1800	1.05×10^3	1.26×10^4	52.2
1783	8.05×10^2	1.02×10^4	39.5
1770	6.73×10^2	8.68×10^3	41.4
1752	6.04×10^2	6.98×10^3	34.4
1741	–	4.74×10^3	22.1
1692	2.60×10^2	2.83×10^3	8.6
1687	2.56×10^2	2.61×10^3	11.7
1683	2.01×10^2	2.54×10^3	8.1
1799	9.71×10^2	1.16×10^4	56.5
1765	5.81×10^2	7.72×10^3	33.8
1713	3.24×10^2	3.81×10^3	12.2
1814	1.10×10^3	1.40×10^4	70.4
1739	4.07×10^2	5.21×10^3	24.7

$(2.40\pm0.36)\ 10^{-8}$ Pa K s^{-1} resulted for the pressure calibration factor used in all runs listed in Table 2.

Partial pressures were evaluated by the use of Eq. (1) for each measuring temperature. Fig. 4 exemplifies the partial pressures of vapor species obtained in run 7 on vaporizing the 8YSZ06Mn sample. Table 4 shows the mean partial pressure equations of the different species evaluated for all samples.

3.4. Thermodynamic activities

Thermodynamic activities of MnO in the samples at 1700 K were determined by comparing their mass spectra with the mean mass spectrum obtained for the samples 8YSZ15Mn and 8YSZ18Mn which consist of the two phases MnO(s) and 8YSZ/MnO solid solution. Activity values of $a(\mathrm{MnO}) > 1$ resulted for the latter two samples if the pure MnO(s) sample was used as reference. The possible explanation for this phenomenon will be discussed in Section 4.

The two independent equilibria

$$\underline{\mathrm{MnO}} = \mathrm{MnO(g)} \tag{2}$$

$$\underline{\mathrm{MnO}} = \mathrm{Mn(g)} + 1/2\mathrm{O_2(g)} \tag{3}$$

were considered in the evaluation of thermodynamic activities. $\underline{\mathrm{MnO}}$ means manganese oxide in the single phase solid solution samples YSZ/MnO(s.s.) or in the two phase reference sample. The following equations result for the computation of the thermodynamic activity of MnO by considering Eq. (1) in addition to the equilibrium constants K°_{p} [Eq. (2)] and K°_{p} [Eq. (3)]:

Table 4
Mean values of the parameters of the partial pressure equation $\ln p(i)/Pa = A/T + B$ for the gaseous species over different $(Zr_{0.85}Y_{0.15})_{1-x}Mn_xO_{1.93-\delta}$ samples

8YSZ l00*x*Mn	No. of runs	ΔT/K	$p(O_2)$/Pa		p(Mn)/Pa		p(MnO)/Pa		$p(i)$/Pa at 1700 K		
x			A	B	A	B	A	B	O_2	Mn(g)	MnO(g)
0.02	1,2	1670–1858	−47383 ±1388	22.402 ±0.811	−43331 ±682	20.960 ±0.372	−51666 ±4639	20.379 ±2.343	4.21×10^{-3}	1.08×10^{-2}	4.48×10^{-5}
0.04	3,4	1668–1838	−45748 ±1140	21.880 ±0.648	−45800 ±307	23.008 ±0.095	−54850 ±3915	23.037 ±2.292	6.54×10^{-3}	1.96×10^{-2}	9.83×10^{-5}
0.06	5,6,7	1683–1851	−42152 ±1349	20.084 ±6.862	−44649 ±835	22.651 ±5.007	−52885 ±3045	22.218 ±1.712	8.99×10^{-3}	2.70×10^{-2}	1.38×10^{-4}
0.08	8,9,10	1661–1810	−39747 ±5205	18.899 ±1.870	−43509 ±1506	22.230 ±0.897	−50192 ±2653	21.147 ±1.663	1.13×10^{-2}	3.46×10^{-2}	2.30×10^{-4}
0.10	11,12,13, 14,15	1539–1797	−36212 ±3024	17.159 ±1.846	−47313 ±5011	24.806 ±3.055	−56702 ±9604	25.670 ±5.574	1.59×10^{-2}	4.85×10^{-2}	4.60×10^{-4}
0.12	16,17,18	1546–1770	−34725 ±4418	16.206 ±2.624	−48556 ±2374	25.823 ±1.589	−58456 ±5264	26.590 ±3.156	1.47×10^{-2}	6.47×10^{-2}	4.11×10^{-4}
0.15	19,20,21	1545–1728	−37157 ±3207	18.075 ±3.330	−52031 ±1064	28.326 ±4.628	−56952 ±1160	26.324 ±2.567	2.28×10^{-2}	1.02×10^{-1}	7.46×10^{-4}
0.18	22,23	1619–1759	−41486 ±3869	20.798 ±2.291	−57337 ±4253	31.136 ±2.596	−59130 ±2333	27.614 ±1.467	2.72×10^{-2}	7.49×10^{-2}	7.71×10^{-4}
MnO(s)	24,25,26	1535–1782	−21064 ±2492	11.461 ±1.598	−64412 ±3098	35.688 ±2.022	−58635 ±3324	27.025 ±1.933	1.08×10^{-2}	1.11×10^{-1}	5.72×10^{-4}

$$a(\mathrm{MnO}) = I(\mathrm{MnO}^+)^{\mathrm{8YSZ/MnO(s.s.)}}/I(\mathrm{MnO}^+)^{\mathrm{Ref.}} \quad \text{and} \tag{4}$$

$$a(\mathrm{MnO}) = \left\{I(\mathrm{Mn}^+)\cdot I(\mathrm{O}_2^+)^{1/2}\right\}^{\mathrm{8YSZ/MnO(s.s.)}}/\left\{I(\mathrm{Mn}^+)\cdot I(\mathrm{O}_2^+)^{1/2}\right\}^{\mathrm{Ref.}} \tag{5}$$

where 8YSZ/MnO(s.s.) and Ref. mean, that the ion intensities were measured over the single phase sample 8YSZ100*x*Mn and over the reference sample [8YSZ/MnO(s.s.) + MnO(s)], respectively.

Table 5 summarizes the thermodynamic activities of MnO in the 8YSZ100*x*Mn samples obtained at 1700 K according to Eqs. (4) and (5). Selected values resulted for each sample composition by taking the average of the values obtained in different runs and by the use of different evaluation procedures. Fig. 5 shows a plot of the selected thermodynamic activities of MnO as function of its concentration in the samples.

4. Discussion

4.1. Vaporization of pure MnO

The initial intention of the investigation of the vaporization of MnO(s) was to study this material as reference for the determination of the thermodynamic activity of MnO in the 8YSZ/MnO solid solution. At the beginning of the mass spectrometric measurement, the MnO(s) sample showed time-dependent ion intensities at constant temperature. This might be caused by small amounts of Mn_3O_4(s) in the sample. Another reason for this phenomenon could be an over-stoichiometry of O in the initial sample which was reduced under low oxygen pressure in the Knudsen cell. This non-stoichiometry of the MnO(s) phase is reported in Refs.[29,30]

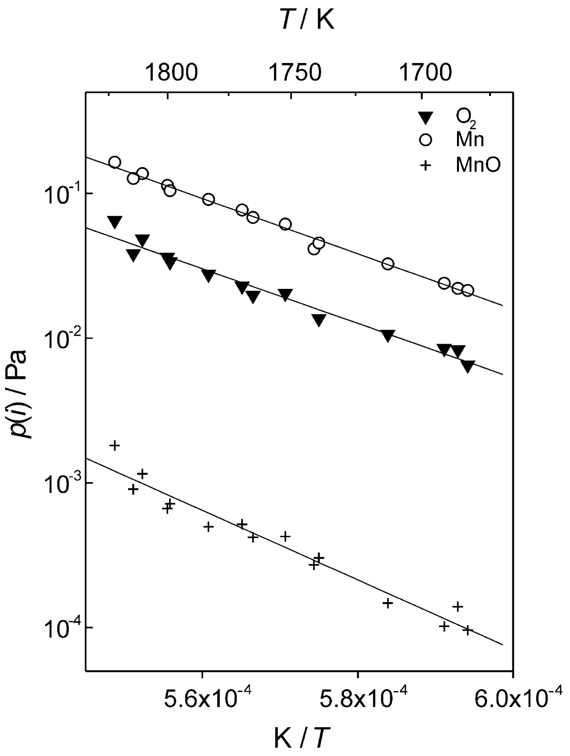

Fig. 4. Partial pressures at different temperatures obtained for the sample 8YSZ06Mn in run 7.

Table 5
Thermodynamic activities of MnO in the $Zr_{0.85}Y_{0.15}0_{1.93}$–$Mn_xO_y$ system at 1700 K determined by the use of Eqs. (2) and (3)

Sample	No. of run	a(MnO), Eq. (2)	a(MnO), Eq. (3)
8YSZ02Mn	1	7.60×10^{-2}	5.01×10^{-2}
	2	4.40×10^{-2}	4.83×10^{-2}
	Selected	$5.46(\pm1.45)\times10^{-2}$	
8YSZ04Mn	3	1.26×10^{-1}	1.07×10^{-1}
	4	1.28×10^{-1}	1.19×10^{-1}
	Selected	$1.20(\pm0.09)\times10^{-1}$	
8YSZ06Mn	5	1.98×10^{-1}	1.82×10^{-1}
	6	1.62×10^{-1}	1.82×10^{-1}
	7	1.75×10^{-1}	$1.79\times q10^{-1}$
	Selected	$1.79(\pm0.12)\times10^{-1}\pm0.01$	
8YSZ08Mn	8	4.22×10^{-1}	3.07×10^{-1}
	9	2.51×10^{-1}	2.57×10^{-1}
	10	2.47×10^{-1}	2.19×10^{-1}
	Selected	$2.84(\pm0.73)\times10^{-1}$	
8YSZ10Mn	11	–	4.30×10^{-1}
	12	–	4.09×10^{-1}
	13	–	3.56×10^{-1}
	14	6.26×10^{-1}	4.70×10^{-1}
	15	5.63×10^{-1}	5.15×10^{-1}
	Selected	$4.36(\pm1.86)\times10^{-1}$	
8YSZ12Mn	16	4.75×10^{-1}	4.61×10^{-1}
	17	5.85×10^{-1}	6.49×10^{-1}
	18	5.39×10^{-1}	5.83×10^{-1}
	Selected	$5.49(\pm0.72)\times10^{-1}$	
8YSZ15Mn	19	9.10×10^{-1}	9.73×10^{-1}
	20	1.02	1.11
	21	1.04	1.18
	Selected	1.04 ± 0.10	
	22	9.30×10^{-1}	8.16×10^{-1}
	23	1.11	9.22×10^{-1}
	Selected	$9.44(\pm1.12)\times10^{-1}$	

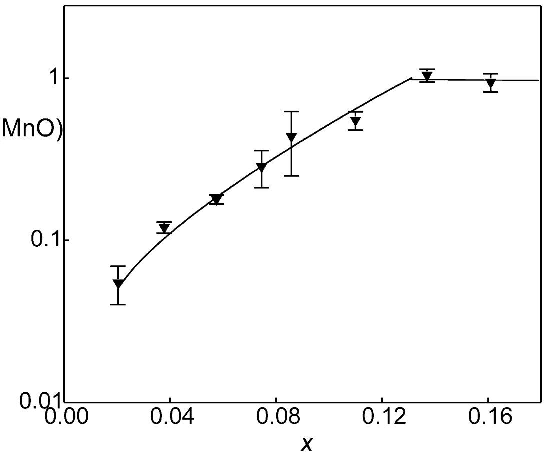

Fig. 5. Thermodynamic activities of MnO in the $(Zr_{0.85}Y_{0.15})_{1-x}Mn_xO_{1.93-\delta}$ samples at 1700 K as a function of the MnO mole fraction, x.

The thermodynamic data obtained in the present study for the vaporization of pure MnO(s) are compared with literature values: The enthalpy change of the reactions Eqs. (2) and (3) was computed according to the second and third law methods. Thermodynamic functions of Mn(g), O_2(g), and MnO(g) were taken from IVTANTHERMO.[31] Enthalpy values of $\Delta H°(298\ K)=532.0\pm39.6$ kJ mol^{-1} (second law) and of $\Delta H°(298\ K)=545.4\pm10.0$ kJ mol^{-1} (third law) were obtained for reaction Eq. (2). The two enthalpy values agree well with the respective value of 546.9 kJ mol^{-1} reported in the IVTANTHERMO compilation.[31] The enthalpy change of reaction Eq. (2) was determined in this work for the first time according to the second law method because it was possible to detect the minor MnO(g) species over a large temperature range. Kazenas et al. [18] obtained the value of $\Delta H°(298\ K)=504.0$ kJ mol^{-1} for reaction Eq. (2) by using only the third law method.

The enthalpy change of reaction Eq. (3) resulted in this work as $\Delta H°(298\ K)=644.1\pm33.4$ kJ mol^{-1} and $\Delta H°(298\ K)=657.1\pm5.6$ kJ mol^{-1} according to the second and third law methods, respectively. The values agree well with values of 668.8 kJ mol^{-1} [31] and 647.6 kJ mol^{-1} [18] reported previously in literature for this reaction.

The enthalpies of the reactions Eqs. (1) and (2) together with the dissociation enthalpy of O_2 ($\Delta H°(298\ K)=498.4$ kJ mol^{-1} [31]) can be used for the evaluation of the atomization energy of MnO(g). The value obtained, $\Delta H°(298\ K)=365.3\pm16.2$ kJ mol^{-1}, agrees excellently with the value determined by Smoes et al. [22] by the use of Knudsen effusion mass spectrometry ($\Delta H°(298\ K)=(368.8\pm7.5)$ kJ mol^{-1}). The two values agree satisfactorily with the dissociation energy of MnO(g) of 385.5 kJ mol^{-1} determined by spectroscopic method in Ref.[32]

4.2. Condensed phase equilibria and partial pressures

XRD and SEM/EDX analysis of the initial samples (Table 1) show, that the 8YSZ100xMn samples with $x \geqslant 0.12$ contained the Mn_3O_4(s) phase in addition to the 8YSZ/MnO solid solution. Chemical analysis of the 8YSZ/MnO solid solution phase in the two-phase samples 8YSZ18Mn and 8YSZ25Mn yielded the solubility limit of Mn in the 8YSZ phase as $x=0.11\pm0.01$ and $x=0.12\pm0.01$, respectively, where x refers to $(Zr_{0.85}Y_{0.15})_{1-x}Mn_xO_{1.93-\delta}$. This confirms the maximum solubility of Mn in 8YSZ of $x=0.11$–0.15 reported in Refs.[12–15] The Mn_3O_4(s) phase containing Mn with the mixed $+2/+3$ valency is stable under the preparation conditions in contrast to MnO(s) used for the sample preparation. As shown in Fig. 3, the Mn_3O_4(s) phase was completely reduced to MnO(s) on studying the sample at high temperature by Knudsen effusion mass spectrometry. Partial pressures of oxygen inside the inert Ir cell result practically only from the dissociative vaporization of MnO thereby being in each case less than 0.1 Pa even at the highest experimental temperatures (s. Table 4). However, according to some investigations,[9,15,16] the Mn atoms dissolved in the 8YSZ phase show also mixed valency at which the $x(Mn^{+3})/x(Mn^{+2})$ ratio depends on temperature and the partial pressure of oxygen.

The 8YSZ12Mn sample showed the two phases 8YSZ/MnO(s.s.) and Mn_3O_4(s) after the preparation and only the phase 8YSZ/MnO(s.s.) after the vaporization study. The probable reason may be the temperature dependent solubility of Mn in 8YSZ or a solubility increase due to the reduction of Mn^{+3} to Mn^{+2}. A further explanation might be the partial depletion of Mn due to vaporization. However, chemical analysis of the samples before and after the vaporization study shows that this depletion was insignificant. In spite of this, depletion of MnO during the vaporization study could be a reason for the differences between data obtained in different runs for the same sample material. The systematic deviation of the Mn-concentration in the samples after preparation from the weighed-in quantities suggests that MnO is depleted during the preparation procedure. The partial pressure data shown in Table 4 should, therefore, be assigned to the mean composition of the solid solution obtained from the Mn concentrations determined by chemical analysis before and after the vaporization study (Table 1).

4.3. Thermodynamic activities

The use of MnO(s) as the reference material for the determination of the MnO-activity in the 8YSZ/MnO solid solution resulted in activity values >1 for the two-phase samples 8YSZ12Mn and 8YSZ15Mn. This might be explained by the mixed +3/+2 valency of Mn in the two phase samples. As mentioned above, YSZ stabilizes the valency +3 for the dissolved Mn. In this case, vaporization of MnO(g) from the 8YSZ/MnO solid solution is described by the reaction

$$\underline{MnO}_{1+\delta} = MnO(g) + \delta/2O_2$$

involving oxygen in addition to MnO(g) and the equilibrium condensed phase. By taking pure stoichiometric MnO(s) as reference, thermodynamic activities > 1 have to be expected for MnO in the 8YSZ/MnO solid solution being in equilibrium with $\underline{MnO}_{1+\delta}$ (samples 8YSZ12Mn and 8YSZ15Mn). For this reason, we choose the two-phase sample {8YSZ/MnO+MnO} as reference material. The thermodynamic activity of MnO obtained in this way shows large positive deviations from ideality in the concentration range investigated, $0.02<x<0.18$.

The thermodynamic activity of MnO in the samples investigated increases from 0.055 for sample $x=0.02$ up to 1 for $x=0.13$ as can be estimated from the graph in Fig. 5. The latter value confirms the solubility limit of Mn in 8YSZ determined in this work by XRD and SEM/EDX.

Diffusion of Mn is observed at the SOFC electrolyte/cathode (8YSZ/$LaMnO_3$) interface which is exposed to air under operating conditions. The $LaMnO_3$(s) phase contains Mn^{+3} on the B-sites of the perovskite.[9,10] The high partial pressure of oxygen at this place should result in a high fraction of Mn^{+3} in the 8YSZ/MnO solid solution. This should hinder the diffusion of Mn from the cathode to the electrolyte if the reduction of Mn^{+3} in the perovskite to Mn^{+2} in the 8YSZ/MnO solid solution is the driving force for the Mn diffusion.[10] This diffusion can be reduced by the admixture of 1–2 mol% of Mn to the electrolyte material 8YSZ at the cathode side resulting in a value for the thermodynamic activity of MnO in 8YSZ of about 0.1 (Fig. 5). The influence of such an admixture on the other important properties of the electrolyte should, however, be checked.

5. Conclusions

Thermodynamic activities of MnO in the 8YSZ/MnO solid solution were obtained experimentally by comparing the vapor pressures over the samples with those obtained for the two-phase sample {8YSZ/MnO+MnO} as a reference. Two independent equilibria were used for the evaluation of the MnO activity. Large positive deviations from ideal behavior result for MnO in the 8YSZ/MnO solid solution.

The solubility limit of MnO in 8YSZ was obtained in the present study as 11±1 mol%. Mn_3O_4(s) (in air) or MnO(s) (at low oxygen pressure) was identified as second phase in addition to the 8YSZ/MnO solid solution in the samples containing larger concentrations of MnO than the solubility limit. The Mn atoms dissolved in the 8YSZ phase show probably a mixed +3/+2 valency with a +3/+2 ratio depending on temperature and oxygen partial pressure.

MnO(s) vaporizes mainly dissociative as Mn(g) and O_2(g). In addition, MnO(g) is present in the equilibrium vapor. The values of the enthalpy change for the vaporization of MnO and for the dissociation of MnO(g) agree well with the literature data. The sublimation enthalpy of MnO(g) was determined in this work for the first time by the use of the second-law method.

Acknowledgements

The authors thank the Deutsche Forschungsgemeinschaft, DFG, and the International Bureau of the German Ministry of Science and Technology for financial support.

References

1. Hannink, R. H. J., Kelly, P. M. and Muddle, B. C., Transformation toughening in zirconia-containing ceramics. *J. Am. Ceram. Soc.*, 2000, **83**, 461–464.

2. Minh, N. Q., Ceramic fuel cells. *J. Am. Ceram. Soc.*, 1993, **76**, 563–588.
3. Steele, B. C. H., Material science and engineering: The enabling technology for the commercialisation of fuel cell systems. *J. Mater. Sci.*, 2001, **36**, 1053–1068.
4. Badwal, S. P. S., Zirconia-based solid electrolytes: microstructure, stability and ionic conductivity. *Solid State Ionics*, 1992, **52**, 23–32.
5. Yoshimura, M., Phase stability of zirconia. *Am. Ceramic Soc. Bull.*, 1988, **67**, 1950–1955.
6. Clausen, C., Bagger, C., Bilde-Soerensen, J. B. and Horsewell, A., Microstructural and microchemical characterization of interface between $La_{0.85}Sr_{0.15}MnO_3$ and Y_2O_3-stabilized ZrO_2. *Solid State Ionics*, 1994, **70/71**, 59–64.
7. Waller, D., Sirman, J. D. and Kilner, J. A., Manganese diffusion in single crystal and polycristalline yttria stabilized zirconia. In *Solid Oxide Fuel Cells V (SOFC V) Vol. 97-18*, ed. U. Stimming, S. C. Singhal, H. Tagawa and W. Lehnert. The Electrochemical Society Proceedings Series, Pennington, 1997, pp. 1140–1149.
8. Kilo, M., Borchardt, G., Lesage, B., Weber, S., Scherrer, S. and Martin, M. *et al.*, Zr and stabilizer tracer diffusion in calcia- and yttria-stabilized zirconia. In *Solid Oxide Fuel Cells VII (SOFC VII) Vol. 2001-16*, ed. H. Yokokawa and S. C. Singhal. The Electrochemical Society Proceedings Series, Pennington, 2001, pp. 275–283.
9. Yokokawa, H., Sakai, N., Kawada, T. and Dokiya, M., Thermodynamic Analysis of Reaction Profiles Between $LaMO_3$ ($M = Ni$, Co, Mn) and ZrO_2. *J. Electrochem. Soc.*, 1991, **138**, 2719–2727.
10. Yokokawa, H., Sakai, N., Kawada, T. and Dokiya, M., Thermodynamic analysis on relation between nonstoichiometry of lanthanum manganese oxide ($LaMnO_3$) perovskites and their reactivity with zirconia. *Denki Kagaku*, 1989, **57**, 829–836.
11. Mitterdorfer, A. and Gauckler, L. J., $La_2Zr_2O_7$ formation and oxygen reduction kinetics of the $La_{0.85}Sr_{0.15}Mn_yO_3$, O_2(g)YSZ system. *Solid State Ionics*, 1998, **111**, 185–218.
12. Kawada, T., Sakai, N., Yokokawa, H. and Dokiya, M., Electrical properties of transition-metal-doped YSZ. *Solid State Ionics*, 1992, **53-56**, 418–425.
13. Mori, M., Abe, T., Itoh, H., Yamamoto, O., Shen, G. Q., Takeda, Y. and Imanishi, N., Reaction mechanism between lanthanum manganite and yttria doped cubic zirconia. *Solid State Ionics*, 1999, **123**, 113–119.
14. Appel, C. C., Zirconia stabilized by Y and Mn: a microstructural characterization. *Ionics*, 1995, **1**, 406–413.
15. Kim, J. H. and Choi, G. M., Mixed ionic and electronic conductivity of $[(ZrO_2)_{0.92}(Y_2O_3)_{0.08}]_{1-y}\cdot(MnO_{1.5})_y$. *Solid State Ionics*, 2000, **130**, 157–168.
16. Yokokawa, H., Sakai, N., Kawada, T. and Dokiya, M., Thermodynamic analysis on interface between perovskite electrode and YSZ electrolyte. *Solid State Ionics*, 1990, **40/41**, 398–401.
17. Marushkin, K. N., Alikhanyan, A. S. and Orlovskii, V. P., The thermodynamic properties of the oxides of zirconium, hafnium, and yttrium. *Zh. Neorg. Khim.*, 1990, **35**, 2071–2077.
18. Kazenas, J. K., Tagirov, W. K. and Zviadatse, G. N., Mass spectrometric investigation of dissociation and sublimation of manganese oxide. *Metallly*, 1984, **5**, 58–59.
19. Tshizhikov, D. M., Tsvetkov, I. V., Kazenas, J. K. and Tagirov, W. K., Dissociation of lower manganese oxides. *Dokl. Akad. Nauk SSSR*, 1973, **208**, 160–162.
20. Hilpert, K., High temperature mass spectrometry in materials research. *Rapid Commun. Mass Spectrom.*, 1991, **5**, 175–187.
21. Stolyarova, V. L. and Semenov, G. A., *Mass spectrometric study of the vaporization of oxide systems*. Wiley, New York, 1994.
22. Smoes, S. and Drowart, J., Determination of the dissociation energies of gaseous iron monoxide and manganese monoxide by the mass spectrometric knudsen cell method. *High Temperature Science*, 1984, **17**, 31–52.
23. Freund, R. S., Wetzel, R. C., Shul, R. J. and Heyes, T. R., Cross-section measurements for electron-impact ionization of atoms. *Phys. Rev. A*, 1990, **41**, 3575–3595.
24. Hilpert, K. & Miller, M., unpublished results.
25. Cooper, J. L. Jr, Pressley, G. A. Jr and Stafford, F. E., Electron–impact ionization cross sections for atoms. *J. Chem. Phys.*, 1966, **44**, 3946–3949.
26. Märk, T. D., Cross section for single and double ionization of N_2 and O_2 molecules by electron impact from threshold up to 170 eV. *J. Chem. Phys.*, 1975, **63**, 3731–3736.
27. *Alladin—a labelled atomic data interface*, http://www.amidis.iaea.org.
28. Drowart, J., Mass spectrometric studies at high temperature. In *Advances in mass spectrometry 1985*, ed. J. F. J. Todd. Wiley, New York, 1986, pp. 195–214.
29. Schuster, D., Dieckmann, R. and Schweika, W., The question of vacancy clusters in manganosit $Mn_{1-\Delta}O$. *Ber. Bunsenges. Phys. Chem.*, 1989, **93**, 1347–1349.
30. Keller, M. and Dieckmann, R., Defect structure and transport properties of manganese oxides: (I) The nonstoichiometry of manganosite ($Mn_{1-\Delta}O$). *Ber. Bunsenges. Phys. Chem.*, 1985, **89**, 883–893.
31. Yungman, V. S., Medvedev, V. A., Veits, I. V. and Bergman, G. A., *IVTANTHERMO- a thermodynamic database and software system for the personal computer*. CRC Press and Begell House, Boca Raton, 1993.
32. Gaydon, A. G., *Dissociation energies and spectra of diatomic molecules*. John Wiley and Sons, New York, 1947.